Highlights of the ATLAS top quark precision measurements

Pavol Bartoš
(Comenius University)
On behalf of ATLAS collaboration

PHENO 2022, 9-11 May, Pittsburgh

Introduction

ATLAS detector

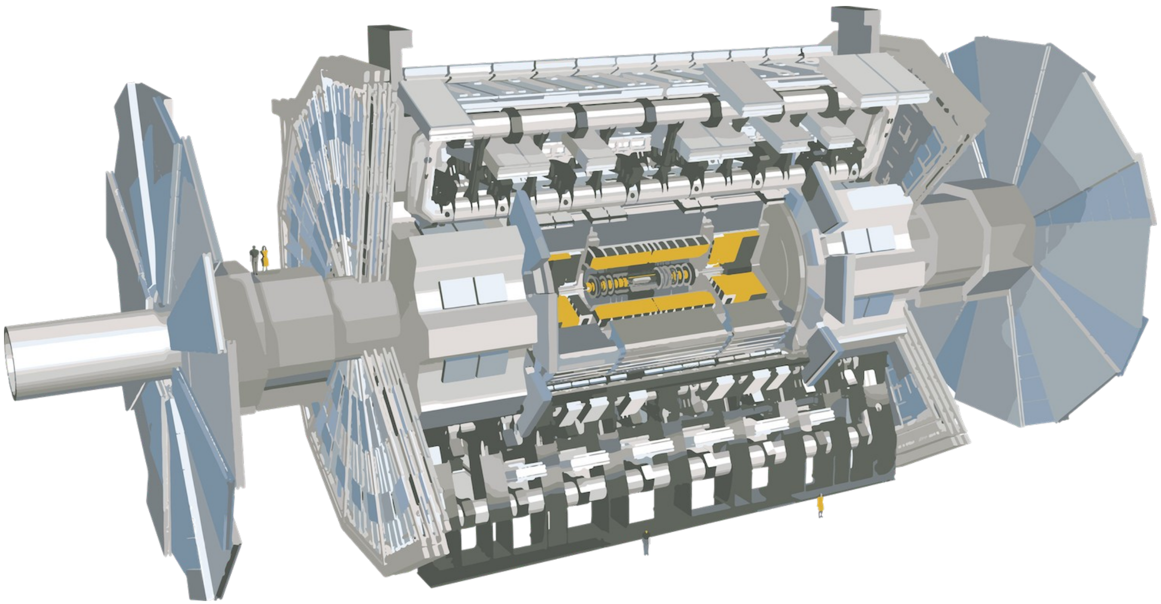

Topics covered in this talk:

- Top quark polarization (single top *t*-channel production)
- Cross-section of top quark pair production (l+jets, all-had decay channels)
- $t\bar{t}$ energy asymmetry
- News from top mass
- Studies with bb4l generator

Why is the top quark so attractive?

- Its large mass (~173 GeV) => short lifetime
- Top decays before hadronization
- Testing of Standard Model (SM) via cross-section measurements
- Top quark mass related to masses of W boson and Higgs boson
- Precise mass measurement – test of electroweak sector of SM

For more top quark related results

see Jiri's talk

visit ATLAS Top WG public web page

Single top quark polarization

Submitted to JHEP, available online: arXiv:2202.11382

t-channel: **top quark** **top antiquark**

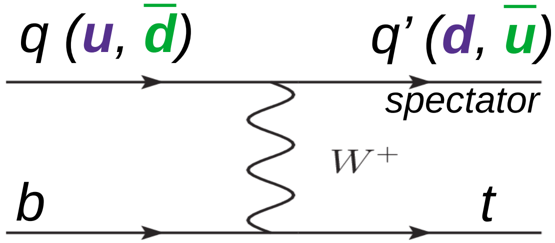

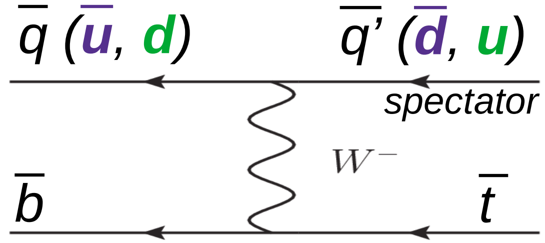

Dominant, **subdominant** process, $\sigma(t)$ / $\sigma(\bar{t}) \approx$ 2:1

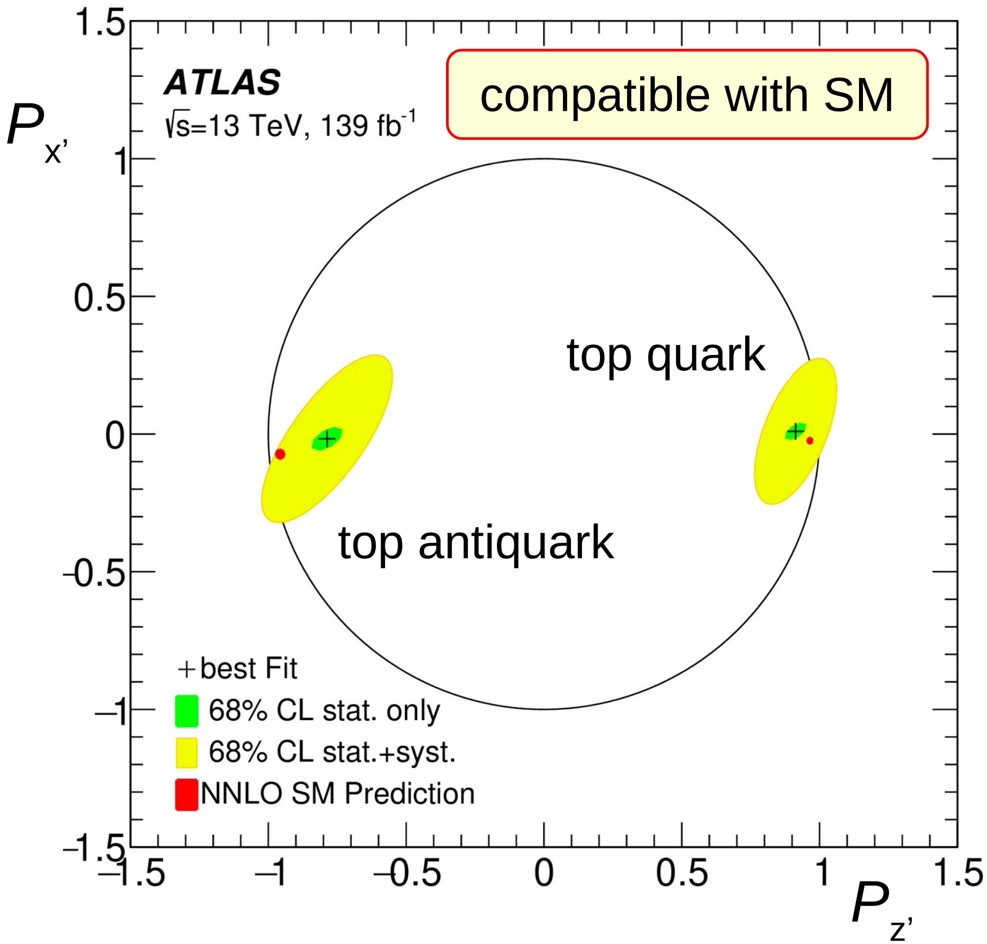

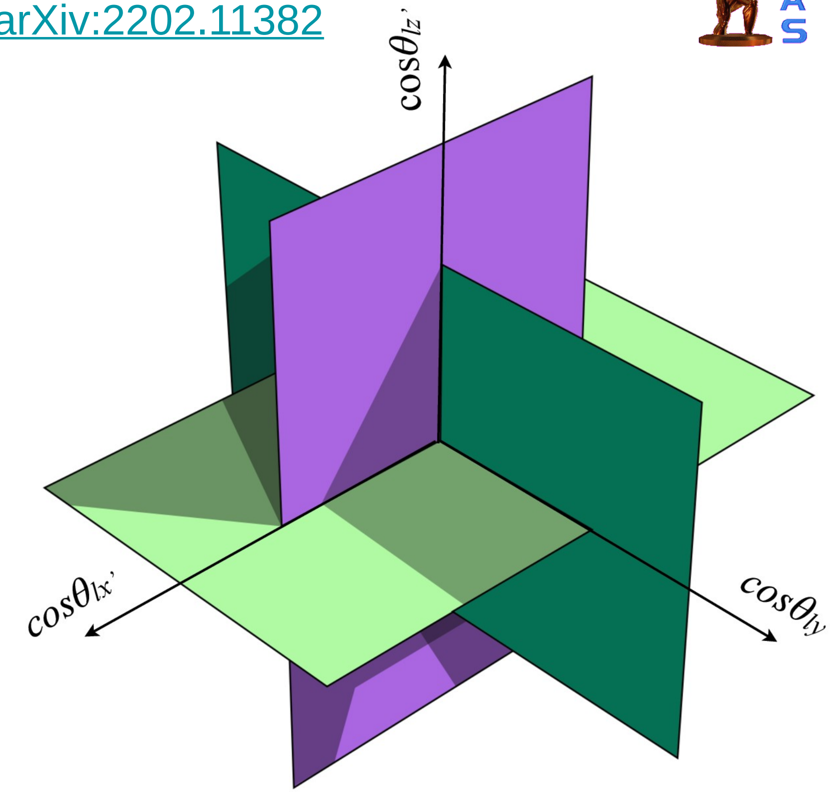

Top quark polarization $P_{x'}$, $P_{y'}$, $P_{z'}$

measurement based on production angle of lepton ($\theta_{lx'}$, $\theta_{ly'}$, $\theta_{lz'}$) in top-quark rest frame

top quark	*top antiquark*
$P_{x'} = 0.01 \pm 0.18$	$P_{x'} = -0.02 \pm 0.20$
$P_{y'} = -0.029 \pm 0.027$	$P_{y'} = -0.007 \pm 0.051$
$P_{z'} = 0.91 \pm 0.10$	$P_{z'} = -0.79 \pm 0.16$

CP symmetry: $P_{y'}(t) = P_{y'}(\bar{t}) = 0$

Single top quark polarization

Submitted to JHEP, available online: arXiv:2202.11382

Differential measurement as function of cosines of lepton production angles

Iterative Bayesian Unfolding used

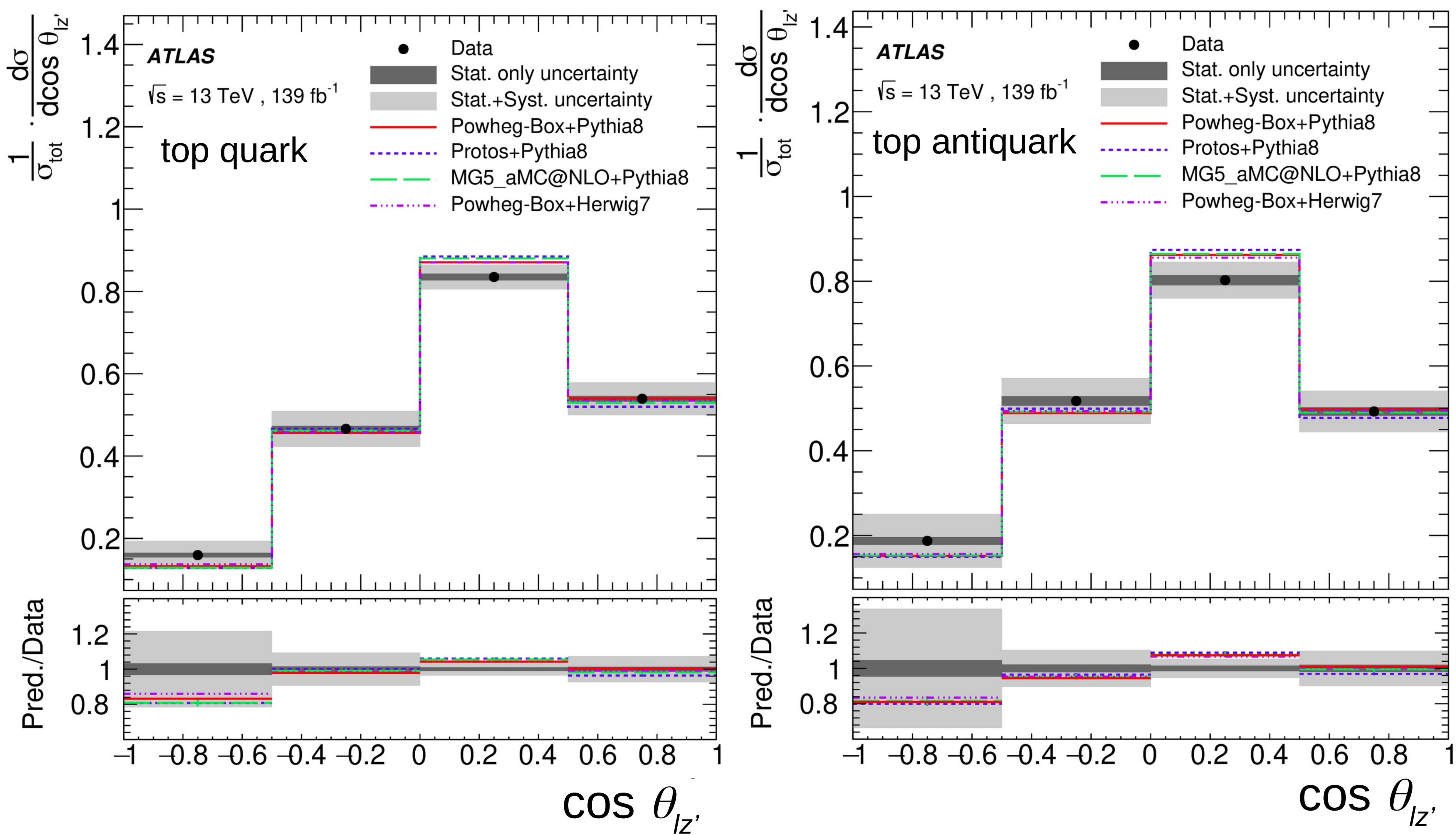

Differential $t\bar{t}$ cross section (l+jets)

Submitted to JHEP, available online: arXiv:2202.12134

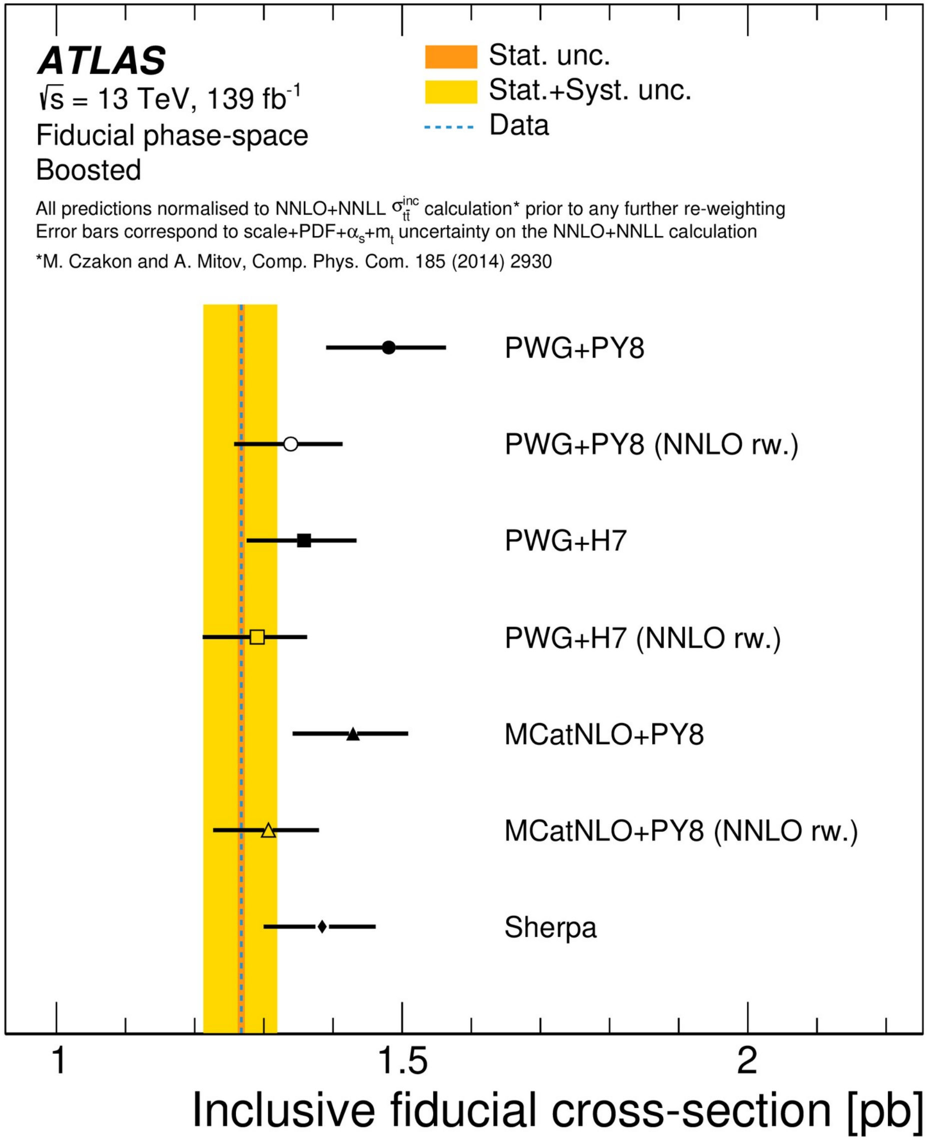

Method:

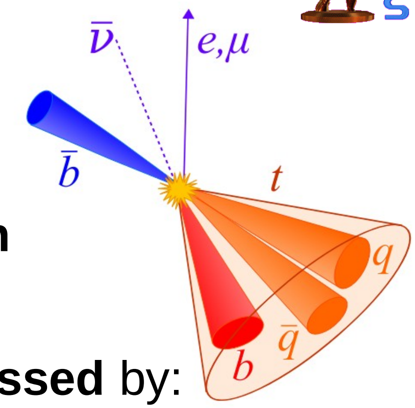

- **mass of large-R jet used** to derive Jet Energy (JES) scale factors **=> reduction of JES systematic**
- **W+jet, single top suppressed** by:
  - ≥ 2 *b*-jets,
  - invariant mass of lepton and *b*-jet to be < 180 GeV
- IBU unfolding to particle level
- Measured in fiducial phase-space
- Differential measurements:
  - Characteristics of top quark kinematic:
    - $p_T^{t,l}$, $p_T^{t,h}$, $|y^{t,l}|$, $|y^{t,h}|$, $m^{t\bar{t}}$, $|y^{t\bar{t}}|$...
  - Probe of additional radiation:
    - $p_T^{t\bar{t}}$, # of additional jets N^j, their p_T , ...
  - 4 two-dimensional measurements:
    - $p_T^{j,1}$ vs $p_T^{t,h}$ (or vs N^j), $\Delta\phi$ (j_1, t_h) vs $p_T^{t,h}$...

Applying parton-level reweighting to match NNLO QCD predictions gives better agreement with data for all generators

Differential $t\bar{t}$ cross section (l+jets)

Submitted to JHEP, available online: arXiv:2202.12134

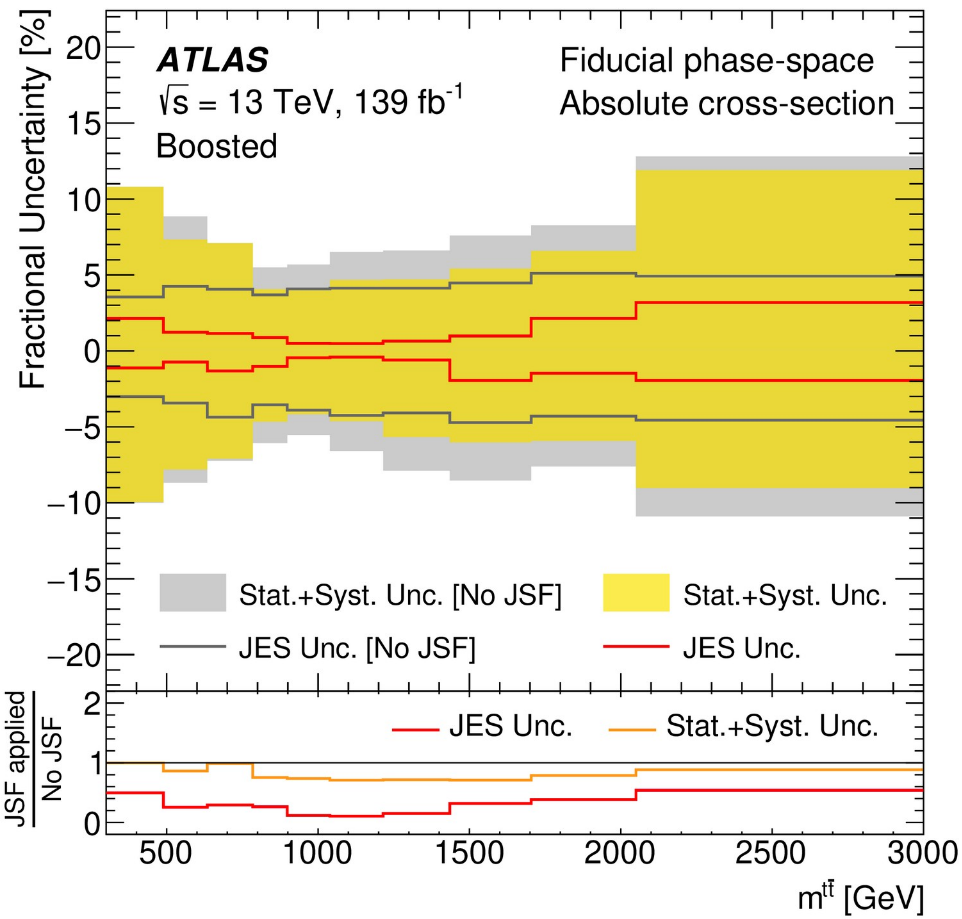

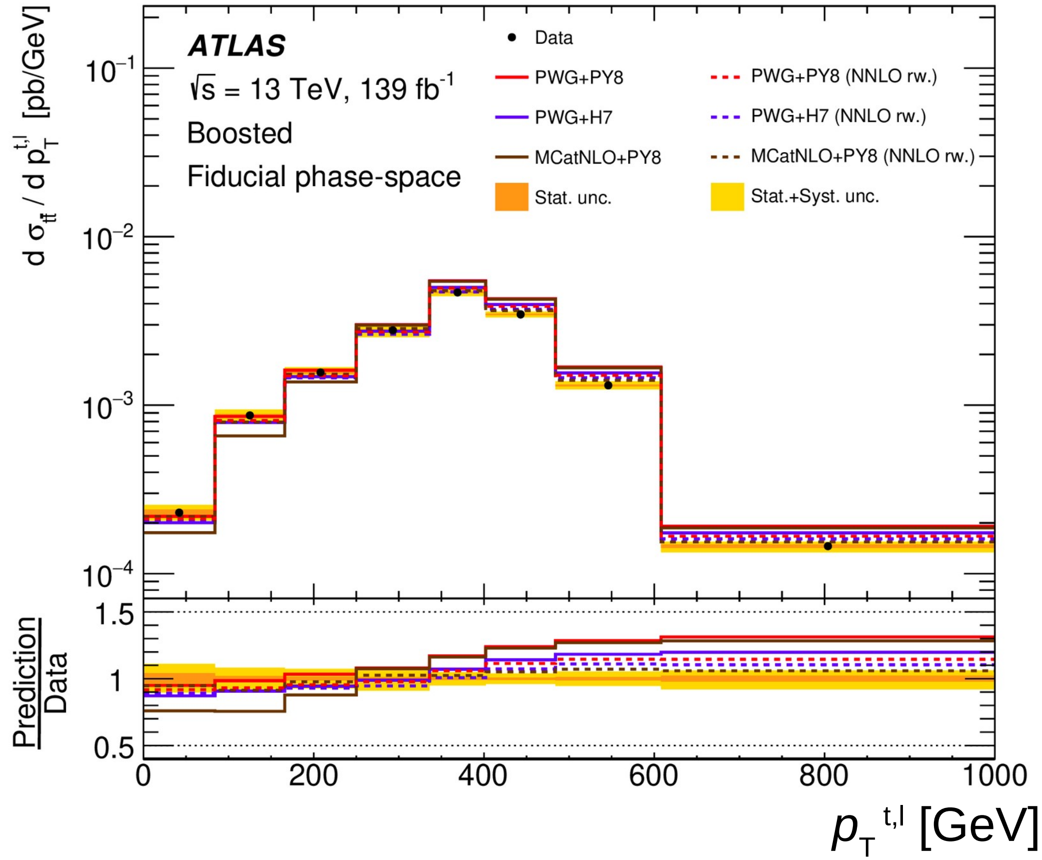

invariant mass of $t\bar{t}$ system

Improvement of uncertainty after using JES scale factors

Transverse momentum of semileptonically decaying top

Improved agreement after applying parton-level reweighting (NNLO rw.) for all generators

Differential $t\bar{t}$ cross section (all-had)

Submitted to JHEP, available online: arXiv:2205.02817

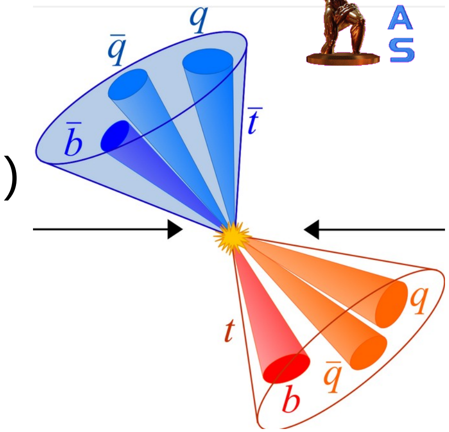

- Single-, double-, triple- differential cross-section
- measured for several variables (p_T, y of top quarks, p_T, y, m of $t\bar{t}$ system, ...)
- Unfolding to particle and/or parton fiducial phase-space
- Uncertainty reduction factor of 2-5 (depending on differential bin) w.r.t previous measurement
- NLO, NNLO prediction obtained from MATRIX program

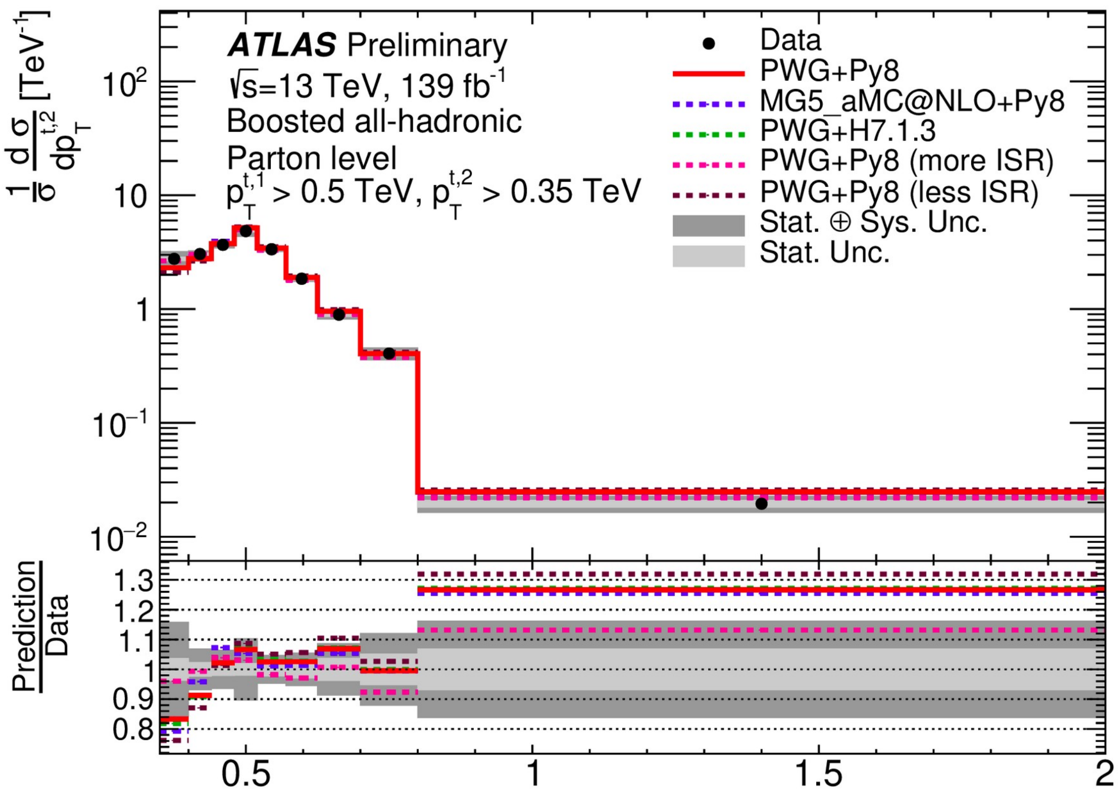

Transverse momenta of second leading top $p_T^{t,2}$ [TeV]

- **Reasonable agreement** found **for** most of the **NLO models**
- Notable **disagreement** of data with NLO + parton shower (PS) predictions **for 2nd leading top p_T**
- Observables sensitive to gluon radiation not well described
- **Agreement with NNLO** at parton level (in general) **better** than with NLO+PS

$t\bar{t}$ energy asymmetry in $t\bar{t}j$ events

Published in: Eur. Phys. J. C 82 (2022) 374

Example of contributions to the energy asymmetry

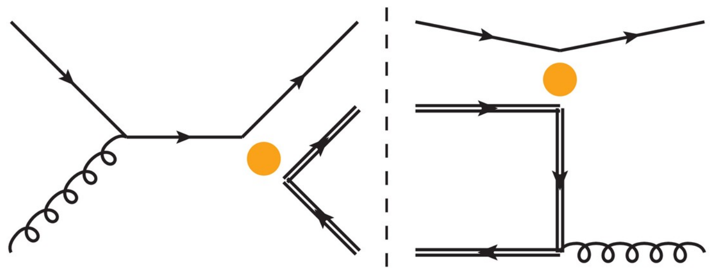

- Double lines ≡ top quarks
- Orange circles ≡ in QCD gluon or four-quark operator in SMEFT (SM effective field theory)

Outgoing quark-jet boosted in direction of incoming valence quark => rapidity of $t\bar{t}j$ system $y_{t\bar{t}j}$ affected

$$A_E(\theta_j) \equiv \frac{\sigma^{\text{opt}}(\theta_j|\Delta E>0) - \sigma^{\text{opt}}(\theta_j|\Delta E<0)}{\sigma^{\text{opt}}(\theta_j|\Delta E>0) + \sigma^{\text{opt}}(\theta_j|\Delta E<0)}$$

σ^{opt} – differential cross section as function of θ_j (production angle of outgoing quark jet)

$\Delta E = E_{\text{top}} - E_{\text{antitop}}$

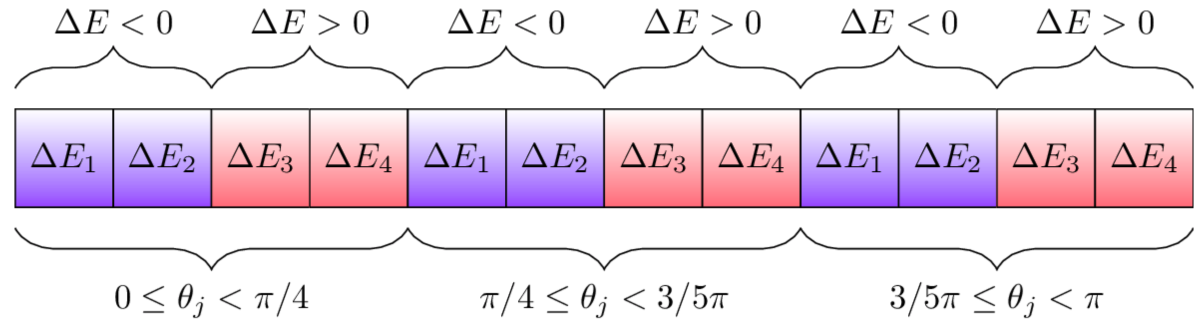

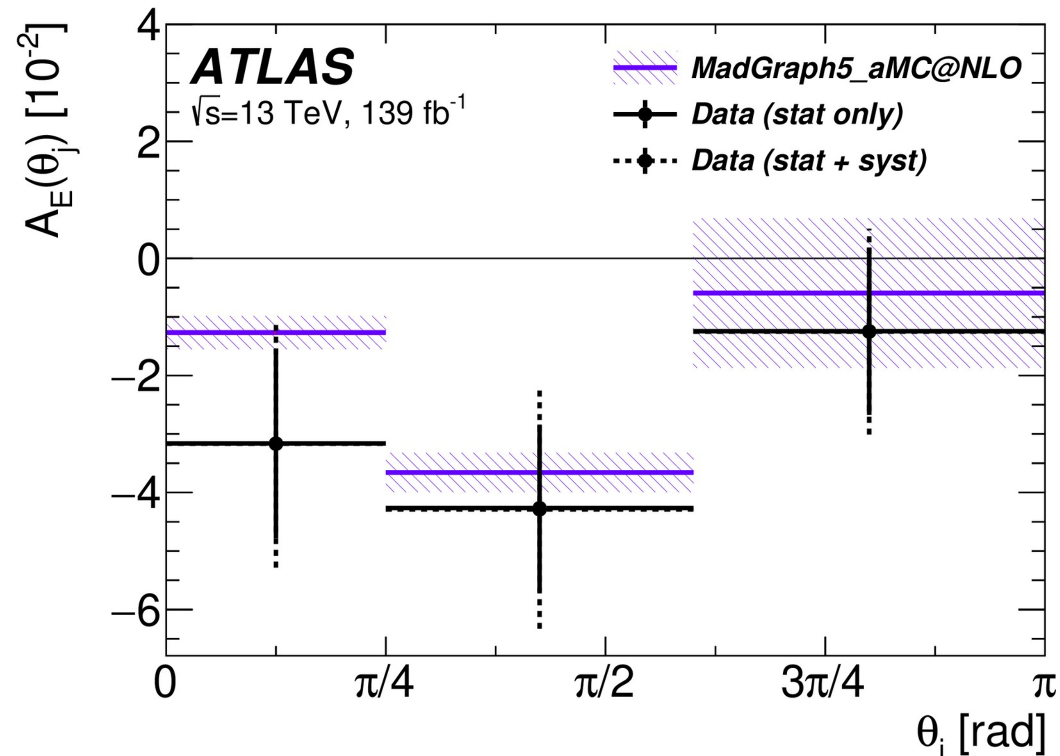

A_E asymmetry is sensitive to the top-quark chirality in four-quark operators => valuable new observable in global SMEFT fits

SMEFT interpretation of results

Published in: ATL-PHYS-PUB-2022-014

Many results provide constraints on Wilson coefficients in SMEFT interpretation

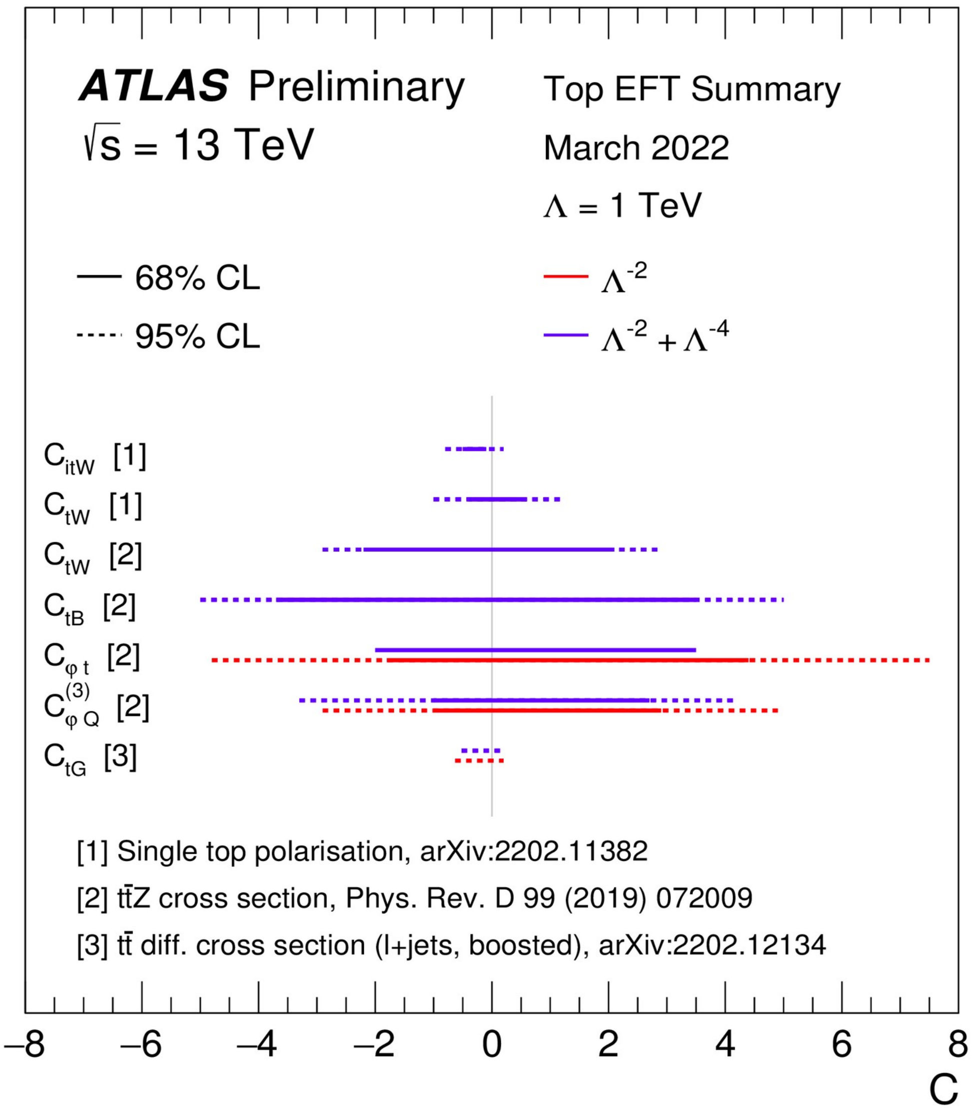

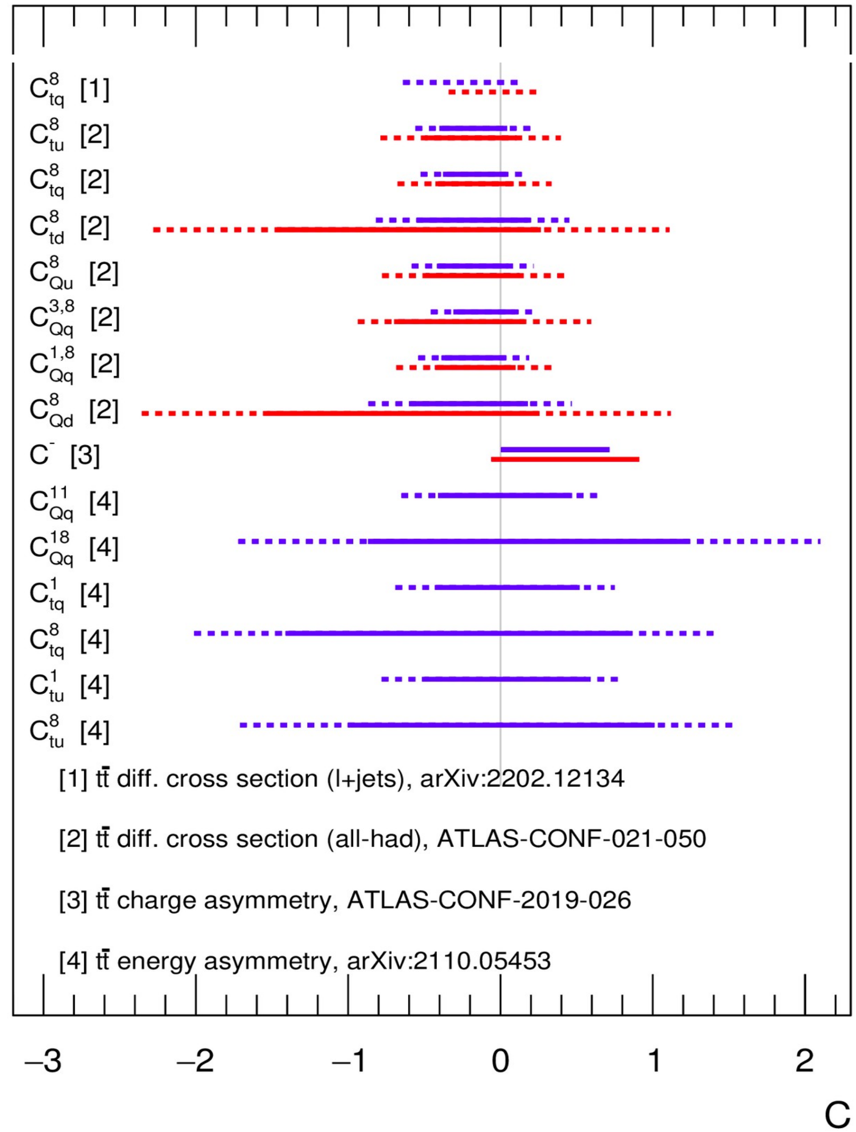

Top mass parameter in MC @ ATLAS

Available online: ATL-PHYS-PUB-2021-034

- Top mass measured in direct measurements using template method

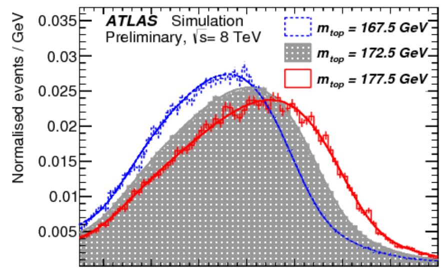

- However top mass parameter m_t^{MC} used by generator **is measured**

- Difference w.r.t. m_t^{MSR} **(1 GeV)** and m_t^{pole} estimated by template method using templates of tree parameters:

  m_t^{MSR} (1 GeV), Ω_{1q}^{∞}, and x_2

  parameters in NLL code affecting hadronization

- Fit is done in 3 bins of top p_T

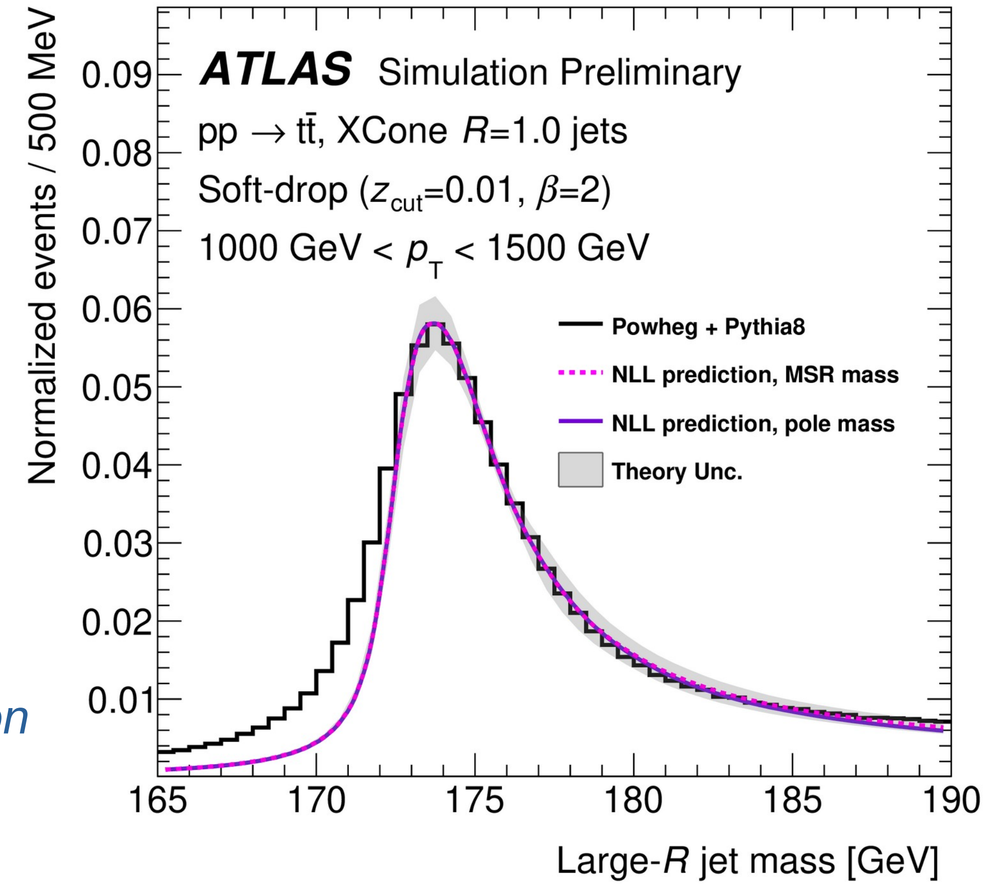

$$m_t^{MC} = m_t^{MSR}(1\,\text{GeV}) + 80^{+350}_{-410}\ \text{MeV}$$

$$m_t^{MC} = m_t^{pole} + 350^{+300}_{-360}\ \text{MeV}$$

Technique based on:

M. Butenschoen et al., “Top Quark Mass Calibration For Monte Carlo Event Generators”

Powheg bb4l generator

Available online: ATL-PHYS-PUB-2021-042

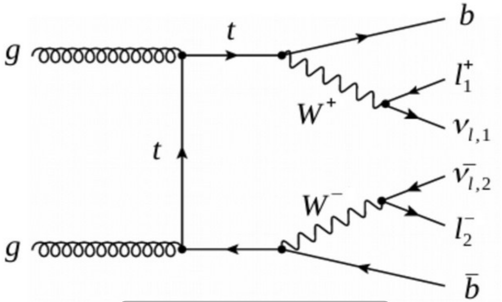

$t\bar{t}$ production

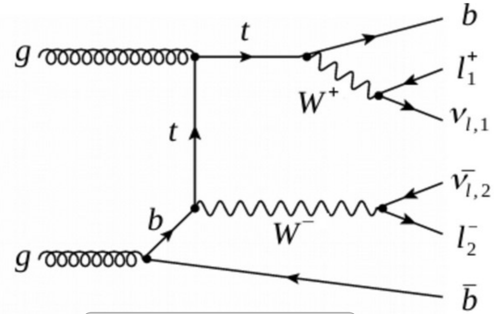

Wt production

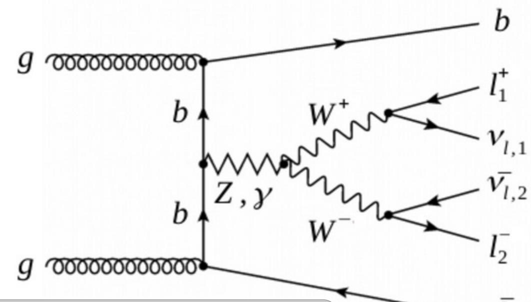

bb4l production (no intermediate top)

Advantages:

- Takes into account quantum interference effects between diagrams with same final state
- Includes off-shell effects
- Top quark decay modelled at NLO

Cons:

- Produce only different flavour dilepton events (*ee*, $\mu\mu$, $\tau\tau$ not included)

Used for multiple studies:

- bb4l compared to simulated $t\bar{t}$ and *Wt* samples with Diagram Removal (DR) and/or Diagram Subtraction (DS)
- template fit of top mass
- Comparison of DR/DS schemes with unfolded dilepton $t\bar{t}$ differential cross-section (next slide)

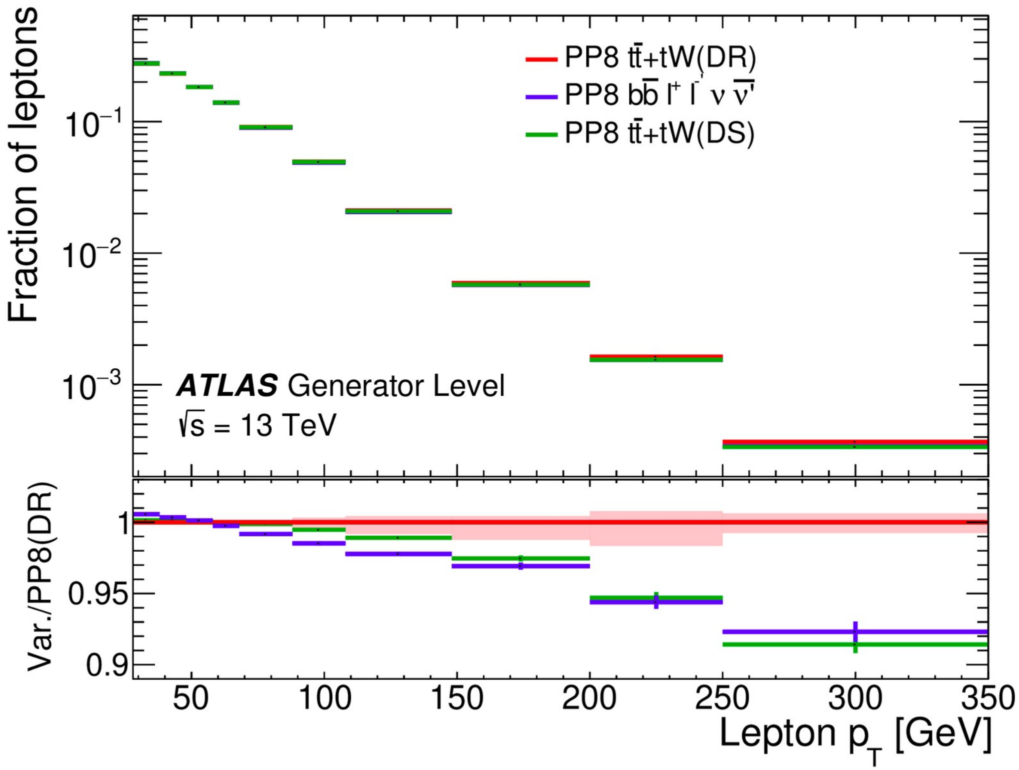

In some distributions bb4l generator agrees better with DS

Powheg bb4l generator

Available online: ATL-PHYS-PUB-2021-042

Comparison of DR/DS schemes with unfolded dilepton $t\bar{t}$ differential cross-section

DR1 vs DR2 – difference in subtraction of double resonant diagrams

DS1, DS2 (**DS3, DS4**) – reshuffling performed on **initial-** (**final-**) state particles

$$m_{b\ell}^{\text{minimax}} = \min\{\max(m_{b_1,\ell_1}, m_{b_2,\ell_2}), \max(m_{b_2,\ell_1}, m_{b_1,\ell_2})\}$$

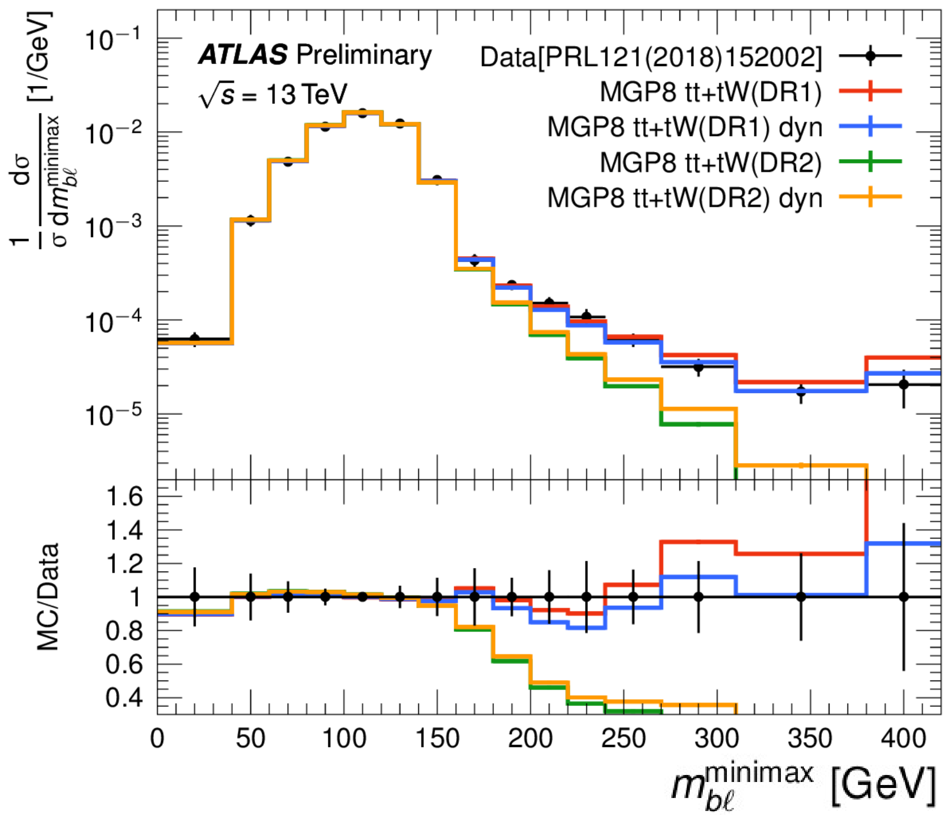

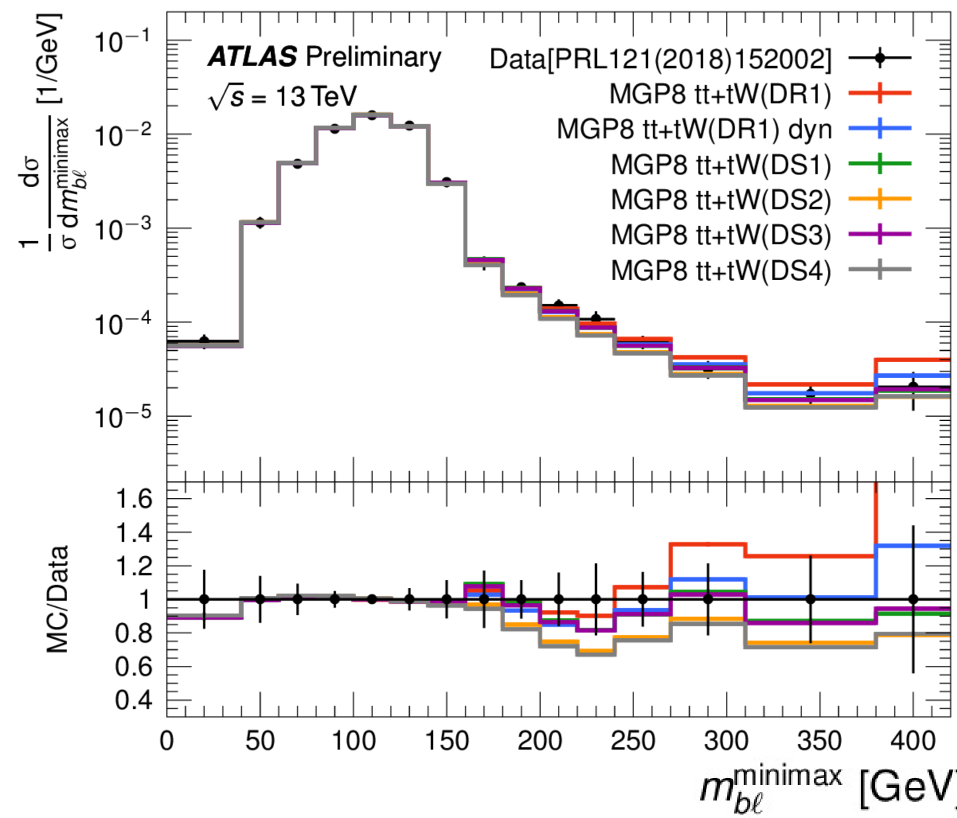

DR2 schemes can be excluded. Dynamic scale choice for the DR1 improves agreement. DS1 and DS3 schemes agree well with data.

Conclusions

- Top quark polarization compatible with SM predictions
- Top-quark pair production measurements with improved sensitivity shows agreement with NNLO better then with NLO
- Energy asymmetry compatible with SM predictions
  → “new kid on the block” for global SMEFT fits
- Constraints on Wilson coefficients in SMEFT interpretation presented
- First step towards understanding relation between top mass parameter in MC and theoretical-well defined top quark mass scheme done
- bb4l generator compared to the currently used MC simulations

More results at: Top-quark physics at ATLAS - public page

Thank you for your attention!

Single top quark polarization

Submitted to JHEP, available online: arXiv:2202.11382

Common event selection criteria			
Exactly one electron or muon			
Veto secondary low-p_T charged loose leptons			
Exactly two jets			
$E_T^{miss} > 35$ GeV			
$m_T(\ell, E_T^{miss}) > 60$ GeV			
$p_T(\ell) > 50\left(1 - \frac{\pi - \lvert\Delta\phi(p_T(j_1), p_T(\ell))\rvert}{\pi - 1}\right)$ GeV			
Preselection region	**Signal region**	**$t\bar{t}$ control region**	**W+jets control region**
Exactly one b-tagged jet	Exactly one b-tagged jet $m_{\ell b} < 153$ GeV $m_{j\ell\nu b} > 320$ GeV Trapezoidal requirement $H_T > 190$ GeV	Exactly two b-tagged jet	Exactly one b-tagged jet $m_{\ell b} > 153$ GeV $m_{j\ell\nu b} < 320$ GeV Veto trapezoidal requirement $H_T < 190$ GeV

Process	Preselection region	Signal region	$t\bar{t}$ control region	W+jets control region
t-channel	219 000 ± 11 000	70 600 ± 3500	13 480 ± 680	148 200 ± 7400
$t\bar{t}$, tW, s-channel	736 000 ± 39 000	43 200 ± 2400	147 800 ± 8400	693 000 ± 37 000
W+jets	590 000 ± 200 000	26 200 ± 8900	16 100 ± 5500	560 000 ± 190 000
Z+jets, diboson	52 900 ± 5100	2120 ± 350	2620 ± 360	50 800 ± 4900
Others	494 ± 38	30 ± 4	79 ± 6	464 ± 36
Multijet	52 000 ± 10 000	3500 ± 640	5500 ± 1800	48 500 ± 9400
Total expected	1 650 000 ± 210 000	145 600 ± 9900	186 000 ± 10 000	1 510 000 ± 200 000
Data	1 750 918	154 361	188 326	1 596 557
S/B	0.15 ± 0.02	0.94 ± 0.13	0.08 ± 0.01	0.11 ± 0.02
Data/Prediction	1.06 ± 0.13	1.06 ± 0.07	1.02 ± 0.06	1.06 ± 0.14

Single top quark polarization

Submitted to JHEP, available online: arXiv:2202.11382

Uncertainty source	$\Delta P^{t}_{x'}$	$\Delta P^{\bar{t}}_{x'}$	$\Delta P^{t}_{y'}$	$\Delta P^{\bar{t}}_{y'}$	$\Delta P^{t}_{z'}$	$\Delta P^{\bar{t}}_{z'}$
Modelling						
Modelling (t-channel)	±0.037	±0.051	±0.010	±0.015	±0.061	±0.061
Modelling ($t\bar{t}$)	±0.016	±0.021	±0.004	±0.016	±0.003	±0.016
Modelling (other)	±0.013	±0.031	±0.003	±0.006	±0.026	±0.043
Experimental						
Jet energy scale	±0.045	±0.048	±0.005	±0.007	±0.033	±0.025
Jet energy resolution	±0.166	±0.185	±0.021	±0.040	±0.070	±0.130
Jet flavour tagging	±0.004	±0.002	<0.001	±0.001	±0.007	±0.009
Other experimental uncertainties	±0.015	±0.029	±0.002	±0.007	±0.014	±0.026
Multijet estimation	±0.008	±0.021	<0.001	±0.001	±0.008	±0.013
Luminosity	±0.001	±0.001	<0.001	<0.001	<0.001	<0.001
Simulation statistics	±0.020	±0.024	±0.008	±0.015	±0.017	±0.031
Total systematic uncertainty	±0.174	±0.199	±0.025	±0.048	±0.096	±0.153
Total statistical uncertainty	±0.017	±0.025	±0.011	±0.017	±0.022	±0.034

Differential $t\bar{t}$ cross section (l+jets)

Submitted to JHEP, available online: arXiv:2202.12134

Object	Detector-level requirements		Particle-level requirements
Leptons	**Exactly 1 lepton in event**		**Exactly 1 lepton in event**
	Electrons	Muons	
	$p_T > 27$ GeV	$p_T > 27$ GeV	$p_T > 27$ GeV
	$\|\eta\| < 1.37$ or $1.52 < \|\eta\| < 2.47$	$\|\eta\| < 2.5$	$\|\eta\| < 2.5$
Small-R jets ($R = 0.4$)	$p_T > 26$ GeV $\|\eta\| < 2.5$		Same as detector-level
b-tagged jets ($R = 0.4$)	DL1r multivariate tagger at 77% efficiency		Jet ghost-matched to b-hadron
	≥ 1 *b*-tagged jet is constituent of top-jet		Same as detector-level
	≥ 1 *b*-tagged jet near lepton: $\Delta R(\ell, b) < 2.0$		
Hadronic top-jet (t, $R = 1.0$) ($R = 0.4$ jets as input)	**≥ 1 top-tagged large-R jet candidate** $p_T > 355$ GeV $\|\eta\| < 2.0$ 120 GeV $< m <$ 220 GeV ≥ 1 b-tagged sub-jet		Same as detector-level
E_T^{miss} & m_T^W	$E_T^{miss} > 20$ GeV $E_T^{miss} + m_T^W > 60$ GeV		Same as detector-level
Electron isolation	$\Delta R(e, t) > 1.0$		Same as detector-level
$m_{\ell b}$	$m_{\ell b} < 180$ GeV		Same as detector-level

Differential $t\bar{t}$ cross section (l+jets)

Submitted to JHEP, available online: arXiv:2202.12134

Source	Uncertainty [%]	Uncertainty [%] (no JSF)
Statistical (data)	±0.4	±0.4
JSF statistical (data)	±0.4	—
Statistical (MC)	±0.2	±0.1
Hard scatter	±0.5	±0.8
Hadronisation	±2.0	±1.8
Radiation (ISR/FSR + h_{damp})	$^{+1.0}_{-1.6}$	$^{+1.4}_{-2.3}$
PDF	±0.1	±0.1
Top-quark mass	$^{+0.8}_{-1.1}$	±0.1
Jets	±0.7	±4.2
b-tagging	±2.4	±2.4
Leptons	±0.8	±0.8
$E_{\text{T}}^{\text{miss}}$	±0.1	±0.1
Pile-up	±0.4	±0.0
Luminosity	±1.8	±1.8
Background modelling	±0.6	±0.6
Total systematic uncertainty	$^{+4.1}_{-4.3}$	$^{+5.8}_{-6.0}$
Total	$^{+4.1}_{-4.3}$	$^{+5.8}_{-6.0}$

Differential $t\bar{t}$ cross section (l+jets)

Submitted to JHEP, available online: arXiv:2202.12134

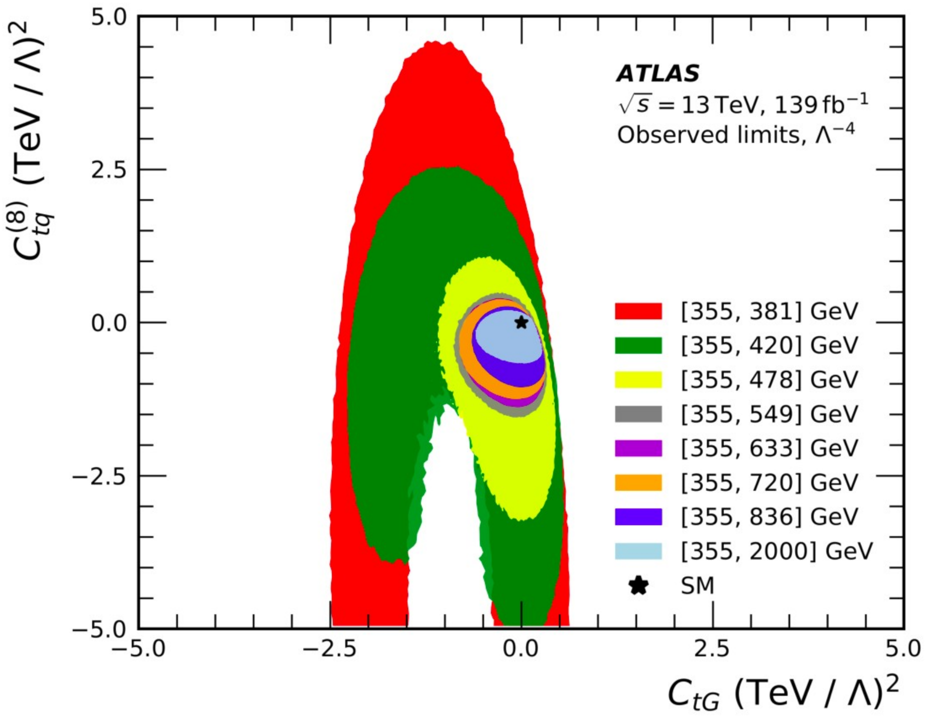

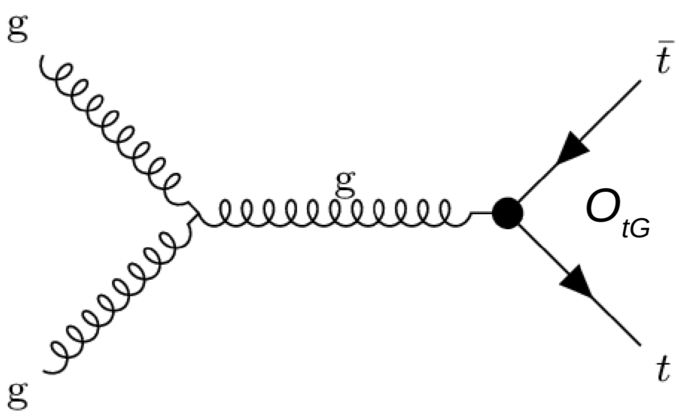

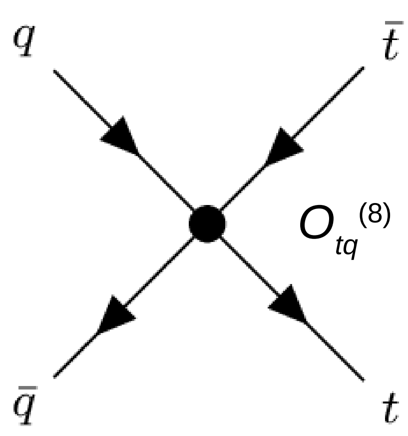

Evolution of the 95% observed credible region when adding the bins of the measured $p_T^{t,h}$

Differential $t\bar{t}$ cross section (all-had)

Submitted to JHEP, available online: arXiv:2205.02817

- triple- differential cross-section

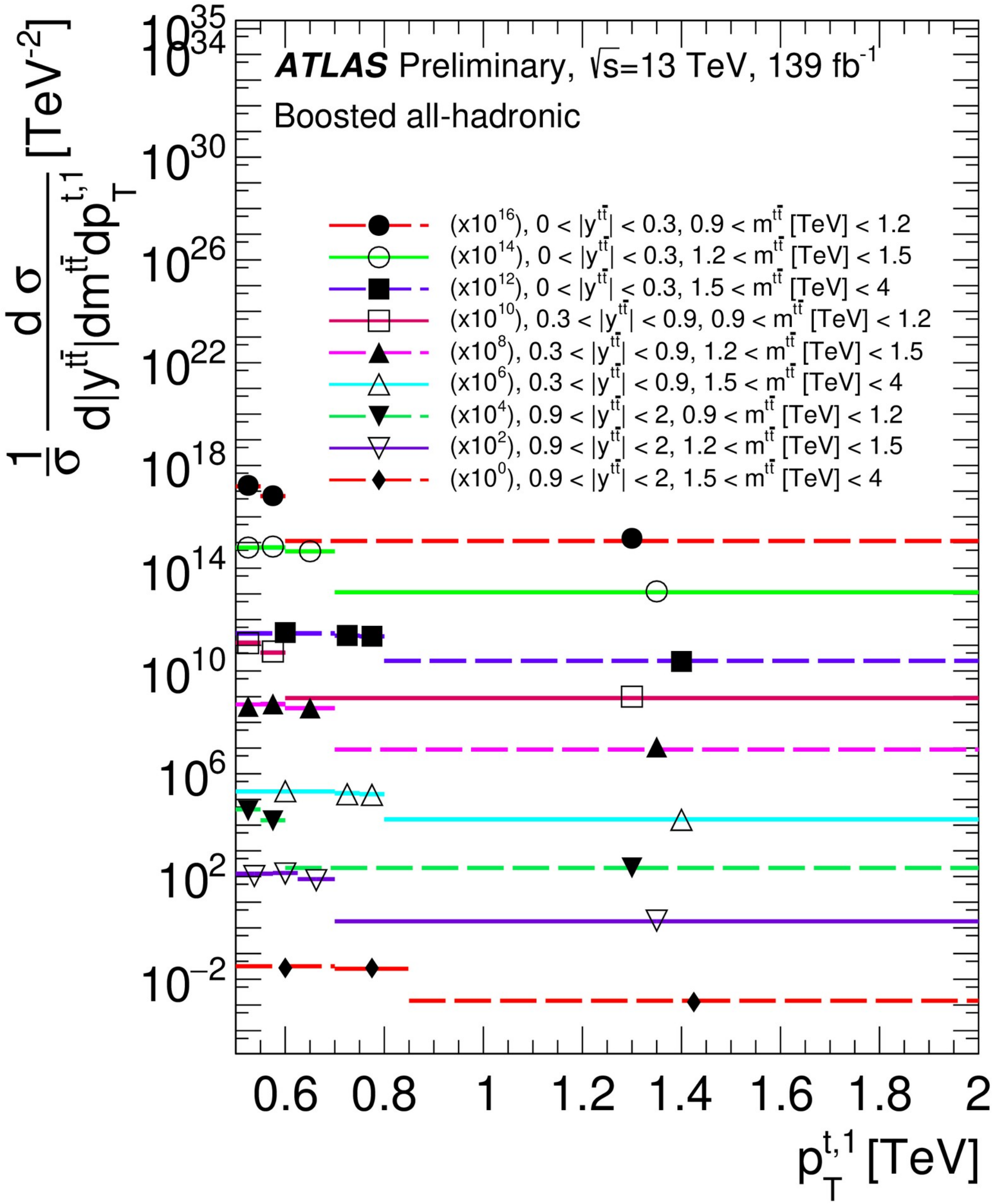

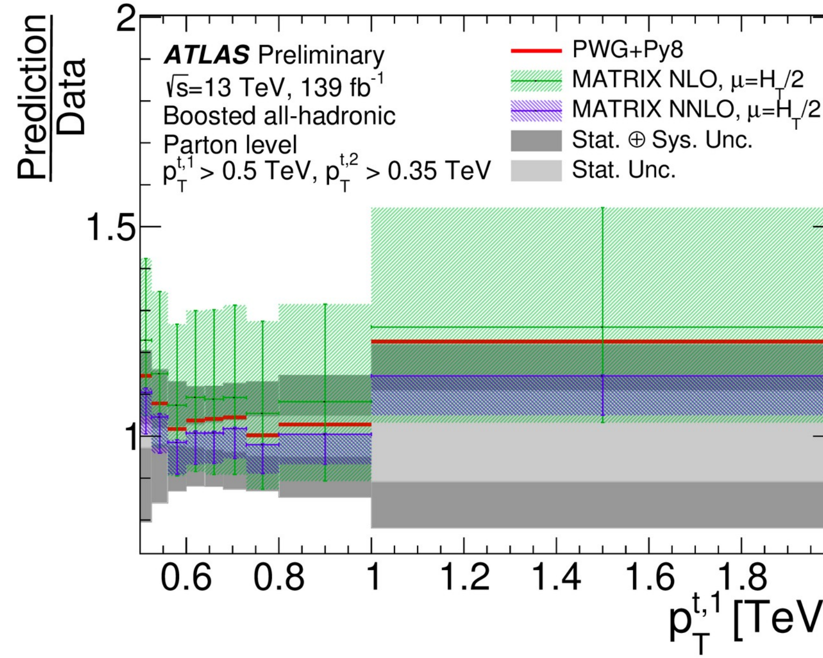

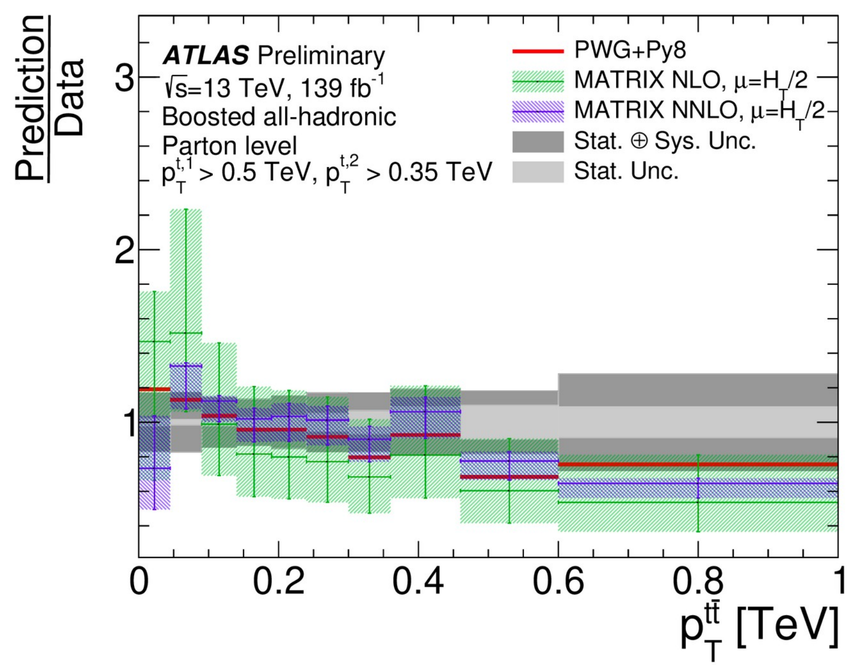

Differential $t\bar{t}$ cross section (all-had)

Submitted to JHEP, available online: arXiv:2205.02817

- Parton level

Source	Relative Uncertainty [%]
Top-tagging	7.8
JES $\oplus$ JER	4.2
JMS $\oplus$ JMR	1.1
Flavor tagging	2.9
Alternative hard-scattering model	5.3
Alternative parton-shower model	2.8
ISR/FSR + scale	5.9
PDF	0.9
Luminosity	1.7
Monte Carlo sample statistics	0.4
Systematics	12.9
Statistics	1.0
Total Uncertainty	13.0

Limits on Wilson coefficients

$C(\text{TeV}/\Lambda)^2$	$\mathcal{O}(\Lambda^{-4})$ 68% CL	$\mathcal{O}(\Lambda^{-4})$ 95% CL	$\mathcal{O}(\Lambda^{-2})$ 68% CL	$\mathcal{O}(\Lambda^{-2})$ 95% CL
$C_{Qq}^{3,8}$	[−0.31 , 0.10]	[−0.46 , 0.25]	[−0.93 , 0.10]	[−1.42 , 0.61]
$C_{Qq}^{1,8}$	[−0.39 , 0.04]	[−0.55 , 0.19]	[−0.47 , 0.08]	[−0.74 , 0.34]
C_{Qu}^{8}	[−0.42 , 0.05]	[−0.59 , 0.22]	[−0.58 , 0.08]	[−0.90 , 0.41]
C_{Qd}^{8}	[−0.58 , 0.18]	[−0.88 , 0.48]	[−1.55 , 0.26]	[−2.43 , 1.13]
C_{tq}^{8}	[−0.38 , 0.03]	[−0.54 , 0.18]	[−0.46 , 0.07]	[−0.71 , 0.32]
C_{tu}^{8}	[−0.40 , 0.04]	[−0.57 , 0.21]	[−0.57 , 0.07]	[−0.88 , 0.38]
C_{td}^{8}	[−0.55 , 0.18]	[−0.83 , 0.46]	[−1.53 , 0.25]	[−2.39 , 1.12]

$t\bar{t}$ energy asymmetry

Published in: Eur. Phys. J. C 82 (2022) 374

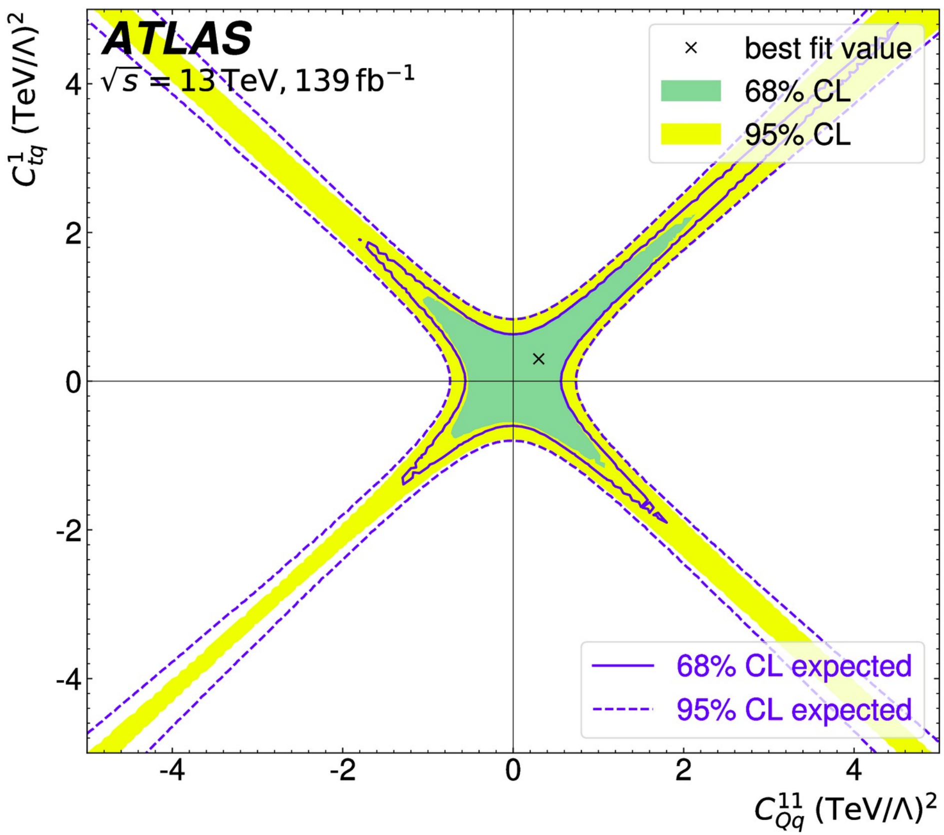

The bounds for colour singlets are generally stronger than for colour octets

Comparison of bounds obtained from
energy asymmetry (green, yellow)
and
bounds obtained from **rapidity asymmetry (blue solid/dashed lines)**

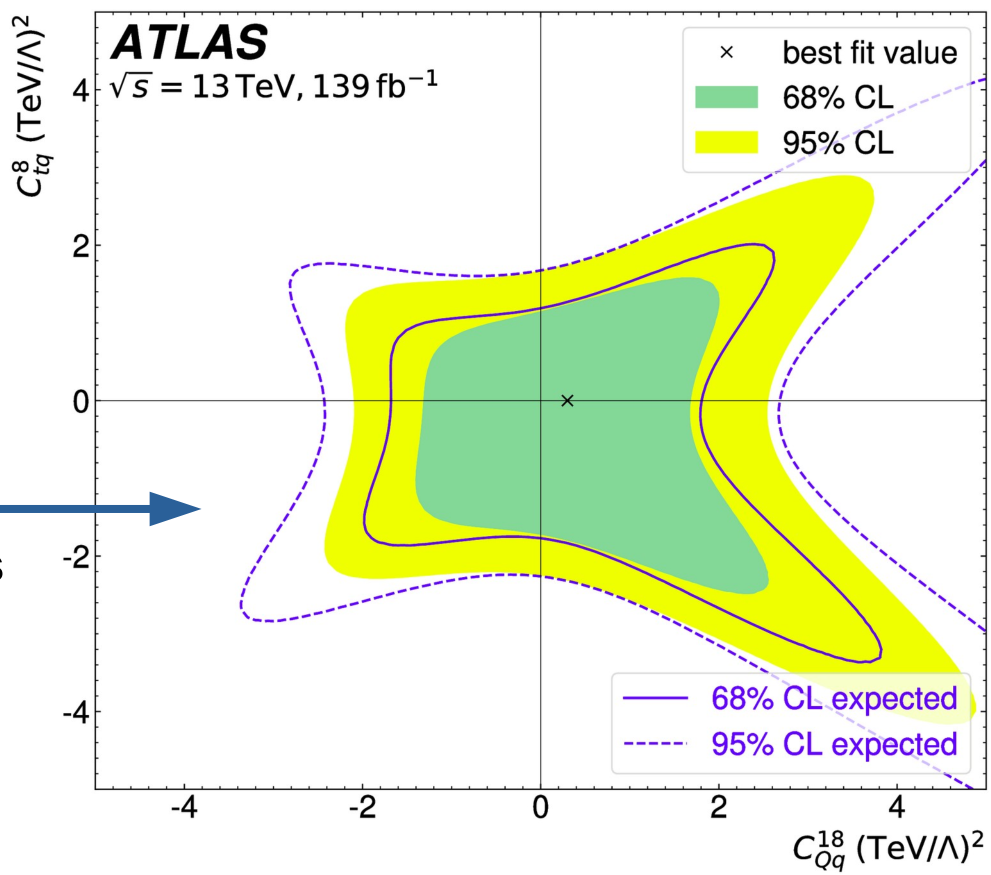

rapidity asymmetry leaves a **blind directions** what is **broken by energy asymmetry** measurement

Top mass parameter in MC @ ATLAS

Available online: ATL-PHYS-PUB-2021-034

$$m_t^{\mathrm{MSR}}(1\ \mathrm{GeV}) = 172.42 \pm 0.10\ \mathrm{GeV}$$
$$\Omega_{1q} = 1.49 \pm 0.03\ \mathrm{GeV}$$
$$x_2 = 0.52 \pm 0.09$$

Source	Size [MeV]	Comment
Theory (higher-order corrections)	$+230/-310$	Envelope of NLL scale variations
Fit methodology	± 190	Choice of fit range, p_T bins
Underlying Event model	± 155	A14 eigentune variations, CR models
Total Systematic	$\mathbf{+340/-340}$	
Statistical Uncertainty	± 100	
Total Uncertainty	$\mathbf{+350/-410}$	

Powheg bb4l generator

Available online: ATL-PHYS-PUB-2021-042

Final state	$t\bar{t}$	$bb4\ell$
Generator	*hvq* [10]	$bb4\ell$ [6]
Framework	POWHEG-BOX	POWHEG-BOX-RES
NLO matrix element	$t\bar{t}$	$b\bar{b}\ell^+\ell^{-'}\nu\bar{\nu}'$
Decay accuracy	LO+PS	NLO+PS
NLO radiation	single	multiple
Spin correlation	approx.	exact
Off-shell $t\bar{t}$ effects	BW smearing	exact
tW and non-resonant effect	no	exact
b-quark massive	yes	yes

NLO generator cross-sections for different DR/DS schemes

Generator	$\mu_\mathbf{R}, \mu_\mathbf{F}$	**DR1**	**DR2**
POWHEG+PYTHIA 8	m_{top}	7.99	—
MADGRAPH5_aMC@NLO+PYTHIA 8	m_{top}	7.98	7.15
MADGRAPH5_aMC@NLO+PYTHIA 8	$H_\mathrm{T}/2$	7.57	6.94

Generator	$\mu_\mathbf{R}, \mu_\mathbf{F}$	**pdf**	**flux**	**DS1**	**DS2**	**DS3**	**DS4**
POWHEG+PYTHIA 8	m_{top}	—	—	7.83	—	—	—
MADGRAPH5_aMC@NLO+PYTHIA 8	m_{top}	true	true	7.68	6.35	7.84	7.68
MADGRAPH5_aMC@NLO+PYTHIA 8	m_{top}	false	true	7.77	7.59	7.79	7.65
MADGRAPH5_aMC@NLO+PYTHIA 8	m_{top}	true	false	7.74	7.26	7.82	7.68
MADGRAPH5_aMC@NLO+PYTHIA 8	m_{top}	false	false	7.72	7.72	7.76	7.63

Powheg bb4l generator

Theory from arXiv:1607.05862

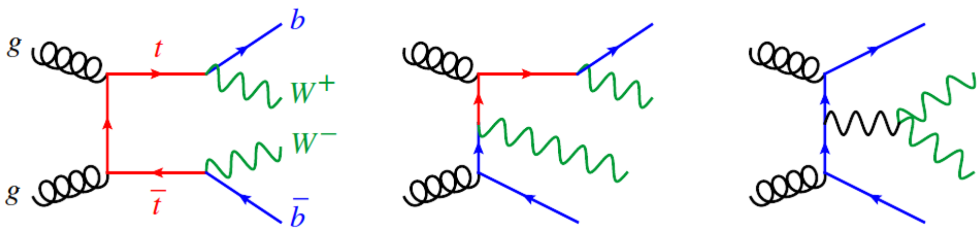

$(\mathcal{A}_{2t})$ $(\mathcal{A}_{1t})$ $(\mathcal{A}_{0t})$

Fig. 2 Examples of doubly resonant (left), singly resonant (center) and non-resonant (right) diagrams contributing to $WbWb$ production. The first two diagrams on the left (with the t line cut) describe the NLO real-emission contribution to the tW^- process.

$$|\mathcal{A}_{tWb}|^2 = |\mathcal{A}_{1t} + \mathcal{A}_{2t}|^2$$
$$= |\mathcal{A}_{1t}|^2 + 2\mathrm{Re}(\mathcal{A}_{1t}\mathcal{A}_{2t}^*) + |\mathcal{A}_{2t}|^2$$

DR1 (no interference term):

$$|\mathcal{A}_{tWb}|^2_{\mathrm{DR1}} = |\mathcal{A}_{1t}|^2 \quad \text{as} \quad \mathcal{A}_{2t} = 0$$

DR2 (with interference term):

$$|\mathcal{A}_{tWb}|^2_{\mathrm{DR2}} = |\mathcal{A}_{1t}|^2 + 2\mathrm{Re}(\mathcal{A}_{1t}\mathcal{A}_{2t}^*)$$

DR is based on removing contributions all over the phase space => not gauge invariant

DS scheme

$$|\mathcal{A}_{tWb}|^2_{\mathrm{DS}} = |\mathcal{A}_{1t} + \mathcal{A}_{2t}|^2 - \mathcal{C}_{2t}$$

$\mathcal{C}_{2t}$, by definition, must

1. cancel exactly the resonant matrix element $|\mathcal{A}_{2t}|^2$ when the kinematics is exactly on top of the resonant pole;
2. be gauge invariant;
3. decrease quickly away from the resonant region.

$$\mathcal{C}_{2t}(\{p_i\}) = f(p_{Wb}^2)\,\big|\mathcal{A}_{2t}(\{q_i\})\big|^2,$$

where $p_{Wb} = (p_W + p_b)$, and $\{p_i\}$ is the set of momenta of the external particles (i.e. the phase-space point), while $\{q_i\}$ are the external momenta after a reshuffling that puts the internal anti-top quark on mass-shell, i.e.

$$\{q_i\} \ : \ q_{Wb}^2 \equiv (q_W + q_b)^2 = m_t^2$$

DS1, DS2 – reshuffling done on initial state particles

DS1:

$$f_1(s) = \frac{(m_t\Gamma_t)^2}{(s-m_t^2)^2 + (m_t\Gamma_t)^2}$$

DS2:

$$f_2(s) = \frac{(\sqrt{s}\,\Gamma_t)^2}{(s-m_t^2)^2 + (\sqrt{s}\,\Gamma_t)^2}$$

DS3, DS4 – reshuffling done on final state particles

Powheg bb4l generator

Available online: ATL-PHYS-PUB-2021-042

Used for multiple studies:

- bb4l compared to simulated $t\bar{t}$ and *Wt* samples with Diagram Removal (DR) and/or Diagram Subtraction (DS)

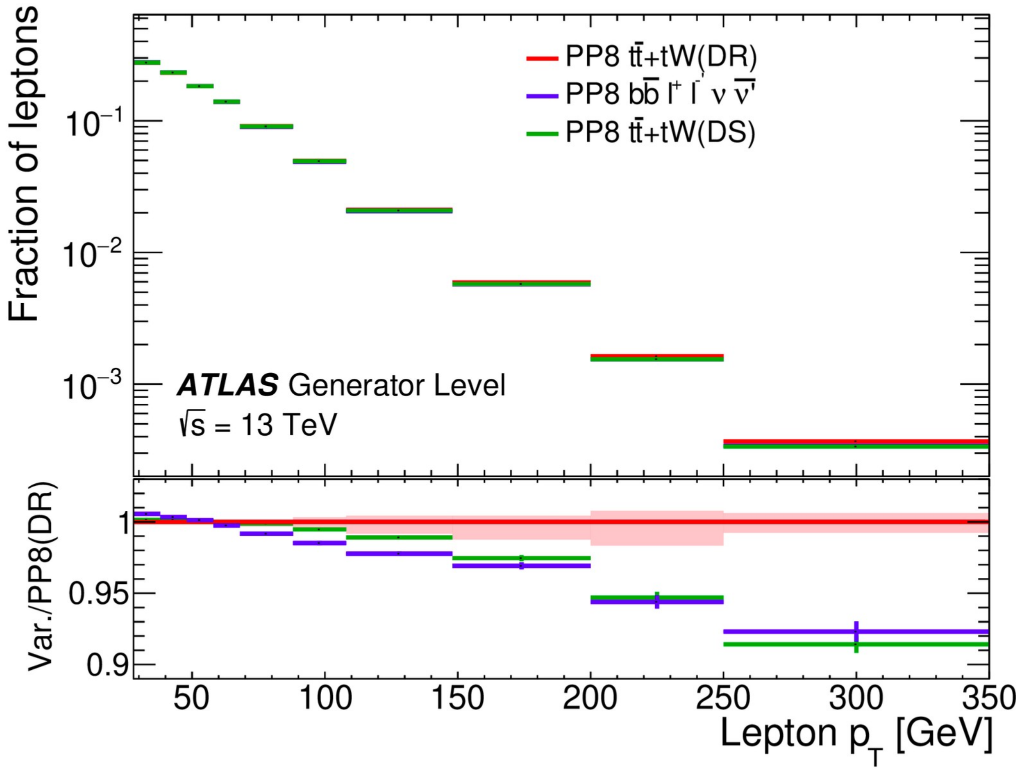

In some distributions bb4l generator agrees better with DS

Used for multiple studies:

- bb4l compared to simulated $t\bar{t}$ and *Wt* (DR) for different h_{damp} and to Powheg+Herwig7

$$m_{\ell b}^{\text{minavg}} = \min\{\frac{m_{\ell_1,b_1} + m_{\ell_2,b_2}}{2}, \frac{m_{\ell_1,b_2} + m_{\ell_2,b_1}}{2}\}$$

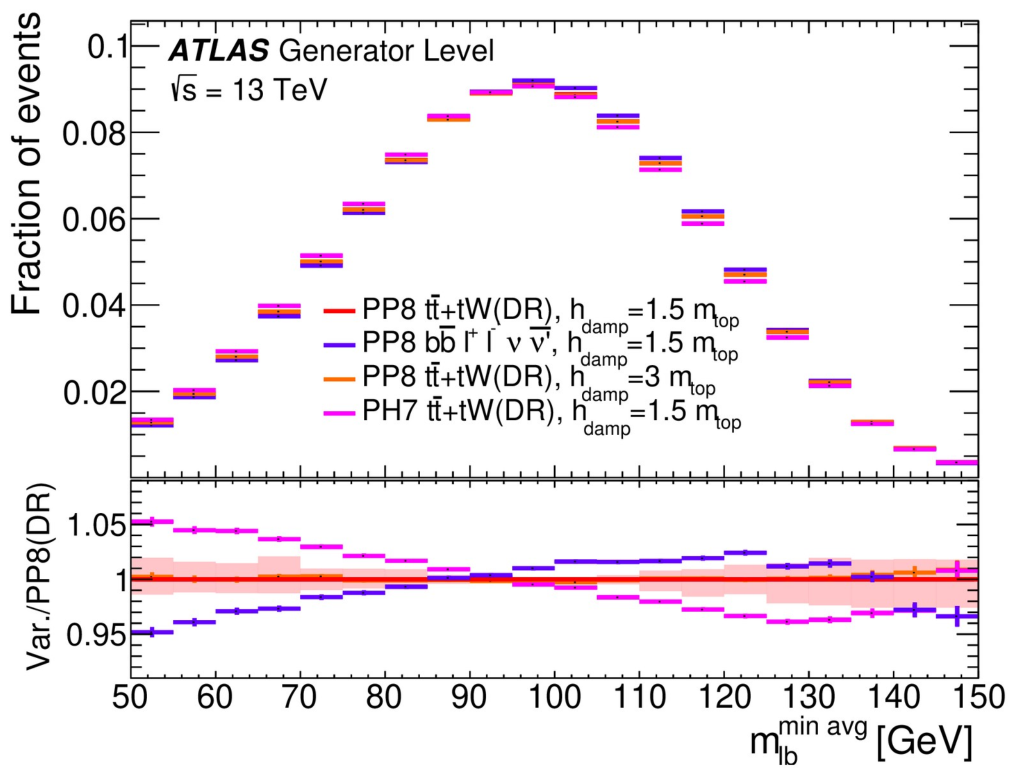

In some distributions bb4l generator opposite effect as Powheg+Herwig7